scientific reports

Check for updates

OPEN

Effects of genetic mutations on left ventricular myocardial mechanics and fibrosis patterns in hypertrophic cardiomyopathy

Minjeong Kim[1,7], Yoonjung Kim[2,7], Hyemoon Chung[3], Jiwon Seo[4], Chul Hwan Park[5], Tae Hoon Kim[5], Se-Joong Rim[4], Kyung-A Lee[2,7]✉ & Eui-Young Choi[4,6,7]✉

Myocyte disarray and fibrosis are underlying pathologies of hypertrophic cardiomyopathy (HCM) caused by genetic mutations. However, the extent of their contributions has not been extensively evaluated. In this study, we investigated the effects of genetic mutations on myofiber function and fibrosis patterns in HCM. A total of 133 patients with HCM underwent chamber geometry, late gadolinium enhancement (LGE), and T1-mapping evaluation using 1.5T cardiac magnetic resonance (CMR) imaging, echo-derived diastolic function analyses, and genetic testing. Left ventricular (LV) segmental and global longitudinal strain (LS), circumferential strain (CS), and rotation were measured using feature tracking analysis. Patients with sarcomere-associated mutation (SM, n = 41) exhibited lower LV-CS (all three slices) and higher basal rotation$_{endo}$, along with a higher prevalence of midepicardial LGE. The relationship between SM and LV-CS$_{myo}$ was independent of LGE amount (ß = 0.239, p = 0.008). However, global LS and E/e' were not correlated with SM but were associated with LV mass index and LGE extent. SM was significantly correlated with the presence of midepicardial LGE (odds ratio 5.81, 95% confidence interval 2.15–15.72, *p* = 0.001), independent of LV mass index, hypertrophy pattern and E/e'. Augmented LV basal segmental rotation was significantly associated with dynamic obstruction. Circumferential fiber dysfunction and midepicardial fibrosis were related to SM, independent of the extent of LV hypertrophy. However, longitudinal fiber function was correlated to the extent of hypertrophy and fibrosis, regardless of SM. Subendocardial fibrosis did not show a significant association with SM.

Keywords Hypertrophic cardiomyopathy, Genetics, Myofiber, Fibrosis

Asymmetrical hypertrophy, myocyte disarray, and fibrosis are underlying pathologies of hypertrophic cardiomyopathy (HCM). Myocyte disarray predominantly occurs in the septum, especially at the junctional site with the right ventricular septum[1]. The cause of myocyte disarray is unclear, although it may be related to genetic mutations in the sarcomere. Regardless of the underlying cause, myocyte disarray leads to inefficient myofiber contraction and relaxation, a feature that, while not specific, is commonly associated with HCM[1,2]. The myocardial fibers roughly comprise longitudinal fibers predominantly located in the subendocardium and circumferential fibers in the mid- to subepicardium. These fibers transit from longitudinal, oblique helical, to circumferential directions, resulting in myocardial deformation[3]. Collectively, these fibers generate counter-clockwise apical rotation and clockwise basal rotation of the left ventricle (LV) viewed from apex, facilitating efficient blood ejection through torsional motion of the LV. However, the effects of sarcomere-associated mutations (SM) on fiber function and hemodynamics have not been thoroughly investigated.

[1]Division of Cardiology, Ewha Woman's University Mokdong Hospital, Seoul, Republic of Korea. [2]Department of Laboratory Medicine, Gangnam Severance Hospital, Yonsei University College of Medicine, 211 Eonju-Ro, Gangnam-Gu, Seoul 06273, Republic of Korea. [3]Division of Cardiology, Kyung Hee University Hospital, Kyung Hee University, Seoul, Republic of Korea. [4]Division of Cardiology, Gangnam Severance Hospital, Yonsei University College of Medicine, Seoul, Republic of Korea. [5]Department of Radiology, Gangnam Severance Hospital, Yonsei University College of Medicine, Seoul, South Korea. [6]Division of Cardiology, Cardiovascular Center, Gangnam Severance Hospital, Yonsei University College of Medicine, 211 Eonju-Ro, Gangnam-Gu, Seoul 06273, Republic of Korea. [7]Minjeong Kim, Yoonjung Kim, Kyung-A Lee and Eui-Young Choi contributed equally to this work. ✉email: KAL1119@yuhs.ac; choi0928@yuhs.ac

Myocardial fibrosis is an important prognostic factor of HCM as it can cause electrical conduction barriers and serve as a potential substrate for fatal ventricular arrhythmias. The extent of fibrosis is utilized as an indicator for implantable cardioverter defibrillator (ICD) implantation[4,5]. Additionally, the extent of fibrosis correlates significantly with LV systolic and diastolic function and can contribute to the progression of HCM to an end-stage condition in certain cases[6]. While patchy midwall late gadolinium enhancement (LGE), especially in the right ventricle (RV) to the septal insertion site, is a typical pattern of fibrosis, various LGE patterns exist in HCM. However, current guidelines for ICD implantation and risk stratification primarily consider the amount of fibrosis rather than its specific patterns[5]. Recent studies have demonstrated an independent association between SM and myocardial fibrosis[7,8]. Nevertheless, the relationship between SM and LGE patterns has not been investigated nor have the hemodynamic effects and myofiber functional changes according to LGE patterns been intensively investigated. Therefore, this study, aimed to investigate the effects of genetic mutations on myofibril mechanics and patterns of LV fibrosis in HCM using cardiac magnetic resonance (CMR) imaging.

Methods

Study population

Among the 212 patients diagnosed with HCM enrolled in this genetic study[9], 133 underwent CMR with LGE imagings. There was no significant difference in clinical characteristics between patients with CMR and without CMR. The patients enrolled in the study had maximal LV hypertrophy ≥ 15 mm or ≥ 13 mm for first-degree relatives, without an underlying cause of hypertrophy, such as uncontrolled hypertension or aortic stenosis[5]. Apical HCM was defined as maximal thickness in apical segments comprising pure type and mixed type. Mixed type was defined as maximal thickness in any apical segments but combined asymmetrical septal hypertrophy below papillary muscle. The inclusion criteria for this study have been previously described in detail[7]. The study protocol was approved by our institutional review board (3-2015-0019), and written informed consent was obtained from each participant. The genetic testing analysis method has been described in detail in previous papers[7,9].

Classification of pathogenic/likely pathogenic sarcomere gene variants

The details are described in Supplemental method.

Echocardiographic analysis

The details are described in Supplemental method.

CMR imaging

CMR was performed using a 1.5-T scanner (Magnetom Avanto; Siemens Medical Solutions, Erlangen, Germany) with a phased array body coil. The LV 2-, 3-, 4-chamber, and short-axis views were obtained using cine images with steady-state free precession (SSFP) sequence. The acquisition parameters were: repetition time (TR) = 55 msec, echo time (TE) = 1.1 msec, flip angle = 67°, 25 phases, slice thickness = 8 mm, slice gap = 2 mm, acquisition matrix = 192 × 109, and field of view = 320 × 400 mm. A bolus of gadolinium-based contrast agent (0.2 mmol/kg gadoterate dimeglumine; Dotarem, Guerbet, France) was intravenously administered at 2 mL/sec, followed by 20 mL normal saline at 4 mL/sec through a 20-gauge cannula in the antecubital vein using a power injector (Nemoto; Nemoto Kyorindo, Tokyo, Japan). After administration of contrast media, LGE imaging was obtained in 10 min, with a fast gradient echo sequence prepared with magnitude- and phase-sensitive inversion recovery (PSIR). The appropriate inversion time before LGE imaging was determined using a fast gradient echo sequence with varied inversion times (150–650 ms) to null the signal from the normal myocardium. The following LGE imaging parameters were used: TR, 8.8 ms; TE, 3.36 ms; flip angle, 25°; acquisition matrix, 256 × 166; and field of view, 276 × 340 mm. Native T1 mapping with a modified Look-Locker technique was performed during the mid-diastolic phase, and post-T1 mapping was performed 15 min after contrast media injection using the same slice axis and parameters as the pre-T1 mapping[10]. Quantitative T2 mapping imaging was performed before contrast media injection with a T2-prepared SSFP pulse sequence along the same short-axis planes used for cine imaging. A motion correction algorithm provided by the vendor was used to reduce motion artifacts.

Measurement of LGE and extracellular volume fraction (ECV)

The presence, patterns, and percentage of LGE in the LV mass were measured using dedicated quantitative analysis software (QmassMR 7.5 or 8.1, Medis, Leiden, Netherland) with Phase-Sensitive Inversion Recovery (PSIR)[11]. LGE patterns were classified as midepicardial (midwall patchy, and subepicardial) or subendocardial (subendocardial or transmural type, so called ischemic pattern) (Fig. 1). Cases with both midwall patchy and subendocardial LGE were classified as midepicardial type. To improve reproducibility, a radiologist and a cardiologist, both with over 10 years of experience, analyzed the LGE sizes. In each short-axis slice image, the boundaries of the contrast-enhanced areas were traced automatically. On LGE-CMR images, the myocardium exhibiting abnormal enhancement was defined as an area of hyperenhancement exceeding five standard deviations from the remote myocardium. The remote myocardium was defined as non-enhanced myocardium, opposite to the hyperenhanced myocardium[12]. The maximal signal was determined using computer-assisted window thresholding of the enhanced area. Obvious artifacts, such as those caused by motion, were excluded using software tools. The total LGE volume was calculated by summing the LGE volumes of all the slices[13]. With QMap and QECV-RE (Medis, Leiden, Netherland), native T1, post-T1, and ECV analyses were performed[7].

Myocardial mechanics with CMR imaging

Myocardial strain analysis was performed using a feature-tracking semiautomated software (Qstrain®MR 2.0, Medis, Leiden, Netherland). The LV endocardial borders were drawn manually in a reference frame. LV

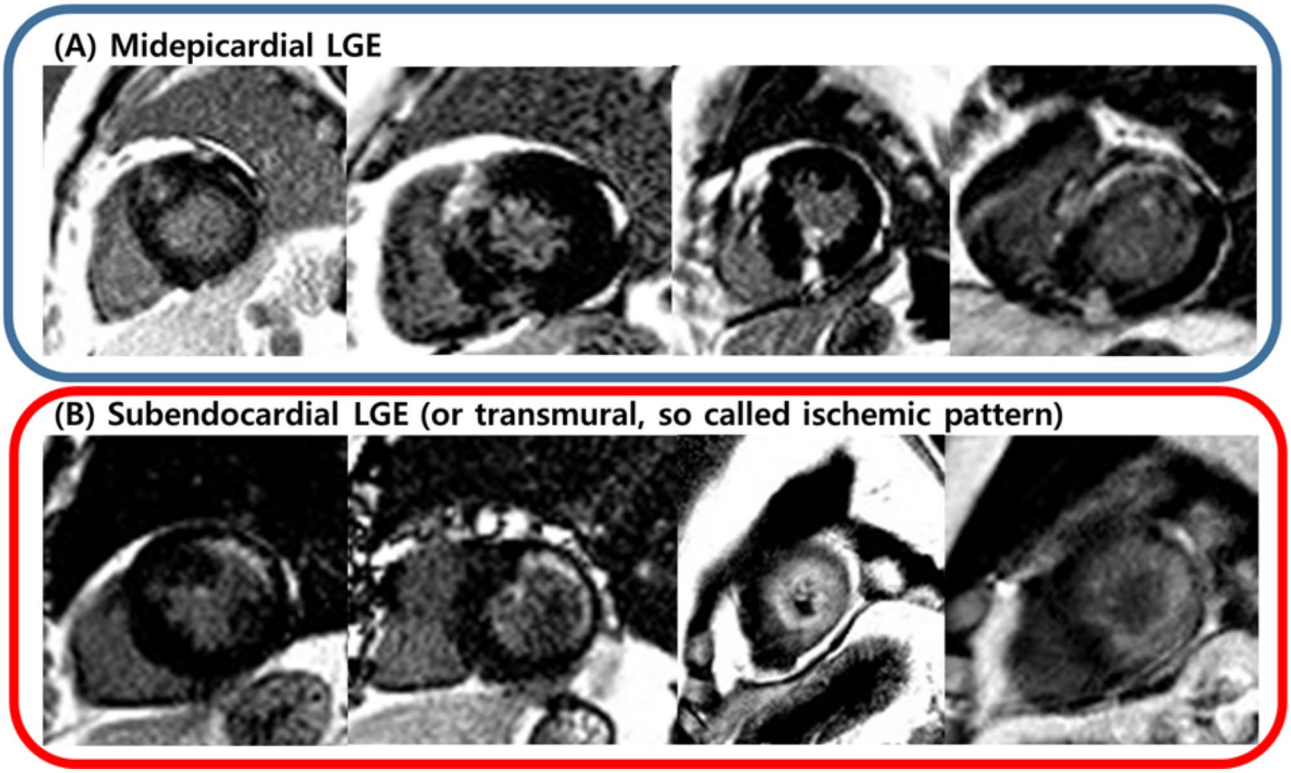

Fig. 1. Late gadolinium enhancement (LGE) pattern in hypertrophic cardiomyopathy. (A) Various cases with midepicardial (midwall and subepicardial) LGE (B) Cases with subendocardial LGE (subendocardial and transmural so called ischemic pattern).

endocardial and epicardial borders were manually traced in 2-, 3-, and 4-chamber long-axis views during both the end-systolic and end-diastolic phases. From these measurements, LV global longitudinal strain (GLS) and segmental longitudinal strains were obtained. The LV basal, mid-, and apical short-axis cine images were used for circumferential strain (CS) and rotation analyses. Each strain value was measured in the endocardium (GLS_{endo}, CS_{endo}, $rotation_{endo}$) and transmyocardium (GLS_{myo}, CS_{myo}, $rotation_{myo}$). Negative number represents clockwise rotation and positive number represents counter-clockwise rotation viewed from apex. The LV twist was calculated as the difference between apical rotation and basal rotation.

Statistical analysis

Continuous variables with normal distributions were presented as mean ± standard deviation (SD) or 95% confidence intervals (CI). Student's t-tests were used to compare the means of normally distributed continuous variables between the two groups. Normality was determined using the Shapiro–Wilk test. Categorical variables were reported as counts (or percentages) and were compared using chi-square test. For comparisons involving more than two groups, an analysis of variance was performed, followed by post hoc analysis using the Fisher's least squares difference test for subgroup comparisons. For the multivariate analysis, linear or logistic regression analyses were performed to check the independence of the variables. Because the %LGE mass and average ECV showed significant collinearity, they were included separately in the multivariable analysis. All statistical analyses were conducted using Statistical Package for the Social Sciences (SPSS) version 25.0 (IBM Corp., Armonk, NY, USA). A two-sided p-value less than 0.05 was considered statistically significant ($p < 0.05$).

Results

Baseline characteristics

The mean age of the participants was 58 ± 13 years, and 35 (26%) of them were women. Among the 133 participants, 34 (26%) had obstructive HCM, while 66 (50%) had apical HCM. The mean values for LV-ejection fraction, LV mass index, and E/e' were 64.7 ± 9.7%, 85.7 ± 22.9 g/m^2, and 14.9 ± 6.0, respectively. Clinical and hemodynamic characteristics according to SM were described in Table 1. The average LV GLS_{myo} was − 16.0 ± 4.2%. The LV-CS_{myo} in basal, mid-, and apical slices were, -19.6 ± 4.0%, -19.5 ± 3.9%, and − 19.5 ± 3.9%, respectively. The average transmural rotation of the basal slice, apical slice, and twist were − 4.65 ± 5.28°, 4.02 ± 8.77°, and 22.6 ± 10.1°, respectively. According to the American College of Medical Genetics and Genomics guidelines[14], 41 (31%) participants had pathogenic or likely pathogenic SMs (19 *MYBPC3*, 12 *MYH7*, 8 *TNNI3*, 2 *MYH6*, 1 *JPH2*, and 1 *TNNC1*). Two patients harbored more than one SMs (one had *MYBPC3* and *MYH7*; another had *MYBPC3* and *JPH2*). Among the 133 patients, 92 (69%) exhibited LGE patterns. Among those with LGE, 73 (79%) patients had

	Patients with SM ($n=41$)	Patients without SM ($n=92$)	P
Age, years	55.9 ± 13.5	59.6 ± 12.8	0.137
Women, n (%)	16 (39)	19 (21)	0.026
Hypertension, n (%)	21 (51)	39 (42)	0.345
Diabetes, n (%)	7 (17)	19 (21)	0.631
Body surface area, m^2	1.75 ± 0.17	1.80 ± 0.20	0.179
Systolic blood pressure, mmHg	118.1 ± 18.0	122.4 ± 19.7	0.233
eGFR, mL/m^2	83.3 ± 15.1	82.5 ± 13.0	0.774
Persistent AF at echo, n (%)	9 (22)	7 (8)	0.019
Apical HCM, n (%)	13 (32)	53 (58)	0.006
LVEF by CMR, %	62.5 ± 9.4	65.7 ± 9.8	0.077
LV mass index by CMR, g/m^2	88.0 ± 21.1	84.7 ± 23.8	0.456
Dynamic obstruction, n (%)	7 (17)	27 (29)	0.134
LA volume index by echo, mL/m^2	41.2 ± 17.6	32.4 ± 11.3	0.005
E/e′	15.4 ± 7.3	14.6 ± 5.3	0.454
Peak TR velocity, m/s	2.4 ± 0.4	2.3 ± 0.3	0.245
ACEI use, n (%)	3 (7)	4(4)	0.479
ARB use, n (%)	18 (44)	46 (50)	0.516
Beta-blocker use, n (%)	25 (61)	67 (73)	0.172
CCB (including DHP) use, n (%)	22 (54)	22 (24)	0.001
Maximal thickness by echo, mm	19.9 ± 3.7	18.4 ± 3.6	0.032
Average anteroseptal wall thickness, mm	13.0 ± 2.9	11.7 ± 3.2	0.025
Average lateral wall thickness, mm	7.6 ± 2.2	8.6 ± 2.2	0.020
Average apical wall thickness, mm	10.5 ± 3.2	10.7 ± 3.9	0.711
LV mechanics			
LV GLS_{myo}, %	− 15.4 ± 4.7	− 16.3 ± 4.0	0.275
LV GLS_{endo}, %	− 18.8 ± 5.9	− 20.2 ± 4.9	0.183
LV average CS_{myo}, %	− 17.89 ± 4.37	− 20.25 ± 3.56	0.001
Basal LV-CS_{myo}, %	− 17.87 ± 4.35	− 20.31 ± 3.68	0.001
Mid LV-CS_{myo}, %	− 17.88 ± 4.38	− 20.23 ± 3.52	0.001
Apical LV-CS_{myo}, %	− 17.91 ± 4.40	− 20.20 ± 3.51	0.002
LV average CS_{endo}, %	− 31.4 ± 7.9	− 35.7 ± 6.4	0.003
Basal LV $rotation_{myo}$, °	− 5.5 ± 4.9	− 4.3 ± 5.4	0.196
Basal LV $rotation_{endo}$, °	− 8.1 ± 9.0	− 4.4 ± 9.2	0.034
Apical LV $rotation_{myo}$, °	1.8 ± 7.4	5.0 ± 9.2	0.055
Apical LV $rotation_{endo}$, °	9.3 ± 20.3	14.4 ± 21.2	0.196
$Twist_{myo}$, °	7.38 ± 9.18	9.25 ± 10.37	0.320
$Twist_{endo}$, °	17.35 ± 24.51	18.77 ± 23.73	0.752
Presence of LGE	37 (90.2%)	55 (59.8%)	< 0.001
Patterns of LGE			< 0.001
Endocardial LGE + transmural LGE	3 (7.3%)	16 (17.4%)	
Midepicardial LGE	34 (82.9%)	39 (42.4%)	
%LGE mass	10.6 ± 10.1	6.8 ± 9.3	0.040
Average native T1, ms	1025.2 ± 46.7	1019.0 ± 49.1	0.512
Average post-T1, ms	579.4 ± 58.6	607.1 ± 63.0	0.021
Average ECV, %	34.2 ± 4.8	31.4 ± 4.3	0.001

Table 1. Baseline clinical, hemodynamic, myocardial mechanistic characteristics, late gadolinium enhacement patterns according to sarcomere-associated mutation. SM, sarcomere-associated mutation; eGFR, estimated glomerular filtration rate; AF, atrial fibrillation; HCM, hypertrophic cardiomyopathy; CMR, cardiovascular magnetic resonance imaging; LV, left ventricular; EF, ejection fraction; LA, left atrial; TR, tricuspid regurgitant; ACEI, angiotensin converting enzyme inhibitor; ARB, angiotensin II receptor blocker; CCB, calcium channel blocker; DHP-dihydropyridine; LGE, late gadolinium enhancement; GLS, global longitudinal strain; CS, circumferential strain; endo, endocardium; myo, transmyocardium; ECV, extracellular volume fraction.

midepicardial LGE, and 19 (21%) patients had subendocardial LGE. Average %LGE mass, native T1 and ECV were 8.0 ± 9.7%, 1020.9 ± 48.3 ms and 32.2 ± 4.6%, respectively.

Myocardial mechanics according to patterns of hypertrophy and fibrosis

Patients with non-apical HCM had a higher LV mass index and a higher average anteroseptal wall thickness. Regarding LV mechanics, LV GLS_{myo} (-15.9 ± 4.7 vs. -16.1 ± 3 .7%, p = 0.045) and LV average CS_{endo} (-33.5 ± 8.3 vs. -35.3 ± 5.6%, p = 0.006) were significantly impaired in non-apical HCM compared to apical HCM. In particular, the average anteroseptal LS was significantly reduced in non-apical HCM (Supplemental Table 1). Regarding patterns of LGE, patients with midepicardial LGE had higher E/e' (16.3 ± 6.5 vs. 12.6 ± 4.7, $p = 0.001$) and LV mass index (91.6 ± 23.3 vs. 73.1 ± 15.5 g/m^2, $p < 0.001$) than the non-LGE group. LV GLS_{myo} in midepicardial LGE was significantly lower than that in the non-LGE group (-15.4 ± 4.5 vs. -17.4 ± 3.8%, $p = 0.019$) but not with the subendocardial LGE group (-15.2 ± 3.7%). Interestingly, basal $rotation_{endo}$ was significantly increased (-7.4 ± 9.1 vs. -3.2 ± 9.7°, $p = 0.022$) and apical $rotation_{myo}$ was significantly decreased (2.1 ± 8.3 vs. 6.6 ± 8.3°, $p < 0.05$) in patients with midepicardial LGE compared to the non-LGE group (Table 2).

Myocardial mechanics and fibrosis pattern according to SM

We repeated strain analysis in 10 cases for GLS, CS and rotation. The intraclass correlation for GLSmyo and CSmyo in the mid slice were 0.971 and 0.952, respectively. For $rotation_{myo}$ and $rotation_{endo}$ in the basal slice, the values were 0.947 and 0.967, respectively; in the apical slice, the values were 0.861 and 0.809, respectively. Patients with SM had a higher average anteroseptal wall thickness, a lower average lateral wall thickness, and a higher prevalence of nonapical HCM. They also exhibited lower average LV CS_{myo} (-17.9 ± 4.4 vs. -20.2 ± 3.6%, p = 0.001) and CSs_{myo} in all three LV slices. However, there were no significant differences in LV mass index, LV ejection fraction, and GLS_{myo} (-15.4 ± 4.7 vs. -16.3 ± 4.0%, p = 0.306) between the two groups. In addition, SM was more closely correlated with higher basal $rotation_{endo}$ (-8.1 ± 9.0 vs. -4.4 ± 9.2°, p = 0.033) compared to others (Table 1). In univariate linear regression analysis, the presence of SM, LGE amount (%), ECV and presence of midepicardial LGE were significantly correlated with a lower average LV-CS_{myo}. In multivariate analysis, SM (ß = 0.239, p = 0.008), LGE amount (ß = 0.267, p = 0.004), ECV were independently correlated with a lower average LV-CS_{myo}. Regarding LV-GLS_{myo}, a higher LGE amount, ECV and LV mass index were significantly correlated with a lower LV-GLS_{myo} but not with SM (Table 3). Patients with SM had a higher prevalence (90% vs. 60%, p < 0.001), amount of LGE (10.6 ± 10.6% vs. 6.8 ± 9.3%, p = 0.04) and ECV. Additionally, patients with SM had a higher prevalence of midepicardial LGE (83% vs. 42%, p = 0.043) but exhibited a lower prevalence of subendocardial LGE (7% vs. 17%, p = 0.021) (Table 1). The midepicardial LGE pattern was significantly correlated to the presence of SM, higher LV mass index, E/e', and nonapical hypertrophy pattern. In the multivariate logistic

	None ($n = 41$)	Mid-epicardial LGE ($n = 73$)	Subendocardial LGE ($n = 19$)	p
Maximal thickness, mm	17.3 ± 2.8	19.9 ± 3.9*	18.2 ± 3.0	< 0.001
E/e′	12.6 ± 4.7	16.3 ± 6.5*	14.3 ± 6.0	0.005
LV mass index by CMR, g/m^2	73.1 ± 15.5	91.6 ± 23.3*	85.7 ± 22.9‡	< 0.001
Average anteroseptal wall thickness, mm	10.2 ± 2.4	13.1 ± 3.3*	12.3 ± 2.3‡	< 0.001
Average lateral wall thickness, mm	8.1 ± 2.0	8.0 ± 2.1†	9.9 ± 2.6 ‡	0.003
Average apical wall thickness, mm	10.1 ± 4.0	10.4 ± 3.2	12.6 ± 4.2	0.038
LV mechanics				
LV EF, %	65.6 ± 7.4	63.9 ± 11.3	66.2 ± 7.4	0.543
LV GLS_{myo}, %	− 17.4 ± 3.8	− 15.4 ± 4.5*	− 15.2 ± 3.7	0.043
Anteroseptal LS, %	− 17.9 ± 3.7	− 15.2 ± 4.4*	− 17.6 ± 5.2	0.003
Lateral LS, %	− 24.6 ± 5.0	− 23.4 ± 6.4	− 22.3 ± 5.1	0.312
Apical LS, %	− 15.4 ± 5.6	− 13.9 ± 5.7	− 11.9 ± 3.7‡	0.070
LV GLS_{endo}, %	− 21.6 ± 4.2	− 19.1 ± 5.7*	− 18.8 ± 4.7	0.032
LV average CS_{myo}, %	− 20.64 ± 3.42	− 18.89 ± 4.38*	− 19.53 ± 2.85	0.075
Basal LV-CS_{myo}, %	− 20.62 ± 3.42	− 18.97 ± 4.52*	− 19.54 ± 2.87	0.110
Mid LV-CS_{myo}, %	− 20.67 ± 3.43	− 18.84 ± 4.33*	− 19.58 ± 2.86	0.059
Apical LV-CS_{myo}, %	− 20.64 ± 3.41	− 18.85 ± 4.34*	− 19.49 ± 2.83	0.066
Basal LV $rotation_{myo}$,°	− 3.6 ± 5.4	− 5.5 ± 5.3	− 3.4 ± 4.8	0.105
Basal LV $rotation_{endo}$,°	− 3.2 ± 9.7	− 7.4 ± 9.1*	− 3.4 ± 7.7	0.040
Apical LV $rotation_{myo}$,°	6.6 ± 8.3	2.1 ± 8.3*	6.0 ± 10.2	0.017
Apical LV $rotation_{endo}$,°	17.0 ± 22.2	10.0 ± 20.3	14.5 ± 20.1	0.220
$Twist_{myo}$,°	10.2 ± 10.6	7.6 ± 9.8	9.4 ± 9.6	0.382
$Twist_{endo}$, °	20.2 ± 26.1	17.4 ± 23.6	17.9 ± 20.9	0.830

Table 2. Comparisons of myocardial mechanics according to patterns of left ventricular fibrosis. See abbreviations in Table 1; LS, longitudinal strain; *, ‡$p < 0.05$ vs. none group; †$p < 0.05$ vs. subendocardial LGE group.

	Average LV-CS$_{myo}$			
	Univariate		Multivariable	
	β	p	β	p
SM	0.276	0.001	0.239	0.008
% LGE mass	0.297	0.001	0.267	0.004
Midepicardial LGE	0.177	0.042	− 0.028	0.773
Average ECV	0.287	0.001	*0.205	*0.032
LV mass index by CMR	0.052	0.555		
Apical HCM	− 0.104	0.236		
	LV-GLS$_{myo}$			
	Univariate		Multivariable	
	β	p	β	p
SM	0.095	0.275		
% LGE mass	0.250	0.004	0.211	0.015
Midepicardial LGE	0.148	0.088		
Average ECV	0.214	0.017	*0.186	*0.035
LV mass index by CMR	0.229	0.008	0.183	0.034
Apical HCM	-0.020	0.822		

Table 3. Relationships between sarcomere-associated mutation and fiber functions. See abbreviations in Tables 1 and 2. *average ECV and %LGE mass were separately included in the multivariable analysis.

	Midepicardial LGE			
	Univariate		Multivariable	
	OR (95% CI)	p	OR (95% CI)	p
SM	6.60 (2.65–16.44)	< 0.001	5.81 (2.15–15.72)	0.001
E/e′	1.11 (1.04–1.20)	0.004	1.08 (0.99–1.18)	0.078
LV mass index by CMR	1.03 (1.01–1.05)	0.002	1.02 (0.997–1.04)	0.103
Apical HCM	0.16 (0.07–0.33)	< 0.001	0.25 (0.11–0.59)	0.001

Table 4. Correlators for midwall late gadolinium enhancement. See abbreviations in Tables 1 and 2. OR, odds ratio; CI, confidence interval.

	LVOT obstruction			
	Univariate		Multivariable	
	OR (95% CI)	p	OR (95% CI)	p
Indexed AML length, per mm/m^2	7.79 (1.43–42.37)	0.018	5.36 (0.93–30.85)	0.060
Maximal thickness, per mm	1.14 (1.02–1.26)	0.017	1.13 (1.02–1.26)	0.022
Basal subendocardial rotation, per 1° clockwise rotation	1.05 (1.01–1.10)	0.025	1.05 (1.004–1.10)	0.034

Table 5. Relationship between basal subendocardial rotation and dynamic left ventricular outflow tract obstruction. LVOT, left ventricular outflow tract obstruction; AML, anterior mitral leaflet.

regression analysis, the presence of any SM was significantly correlated with the presence of midepicardial LGE (odds ratio [OR] 5.81, 95% CI 2.15–15.72, $p = 0.001$), independent of LV mass index, hypertrophy pattern (apical HCM vs. nonapical HCM), and E/e' (Table 4).

Hemodynamic effects of myocardial mechanics and fibrosis

The presence of LV outflow tract (LVOT) obstruction was significantly correlated with the indexed anterior mitral leaflet (AML) length, maximal thickness and the degree of basal rotation$_{endo}$. In multivariate analysis, augmented basal subendocardial rotational motion was significantly correlated (OR 1.05, 1.00–1.09, p = 0.049) with the presence of LVOT obstruction independent of indexed AML length and maximal thickness (Table 5). Regarding diastolic function assessed by E/e', a higher LV mass index (ß = 0.251, $p = 0.003$), LGE amount (ß = 0.169, $p = 0.043$), and presence of LVOT obstruction (ß = 0.191, $p = 0.021$) were significantly and independently correlated with a higher E/e' but not with the presence of SM (Supplemental Table 2).

Discussion

In our study, we observed a significant impairment in circumferential fiber function in patients with SM, independent of fibrosis amount and the degree of LV hypertrophy. This finding suggests that circumferential fiber dysfunction is an independent phenotype associated with the genetic mutation. However, longitudinal fiber function was primarily affected by LV hypertrophy and fibrosis, but not by SM in HCM. The patterns of fibrosis, especially the midwall patchy LGE, were significantly and independently associated with SM. Moreover, we observed that dynamic LVOT obstruction was related to augmented LV basal rotation, independent of maximal thickness and elongated AMLs. This suggests that LV basal rotation can be a primary target of myosin inhibitors. Additionally, we found that LV diastolic function was more strongly related to LV mass, the extent of fibrosis, and the presence of dynamic LVOT obstruction, regardless of SM.

Circumferential fiber dysfunction as an independent phenotype of HCM

HCM is related to the over-activation of actin-myosin binding properties at the molecular level owing to SMs, such as *βMYH7* and *MYBPC3*[15]. However, at the cellular level, myocyte disarray is one of the commonly associated phenotypes in HCM that results in myofibrillar dysfunction[1,2,16]. Among the different myofibrils, the longitudinal myofibril is primarily located in the subendocardium, whereas the circumferential myofibril is located in the midepicardial wall. These myofibrils play distinct roles in the longitudinal and circumferential contraction of the myocardium, respectively[3]. In fact, the transition from longitudinal fiber to circumferential fiber occurs gradually across the myocardial wall, and the combined torque generated by these fibers results in counterclockwise rotation in the apical segment and clockwise rotation in the basal segment of the LV. Previous pathologic studies have identified that HCM is primarily a disease of the midmyocardium, where the circumferential fiber is the main component[1]. The myocyte disarray is usually located in the mid-myocardium, particularly at the septal-RV insertion sites[1]. In our study, the LV-CS was significantly lower in the mutation-positive group, despite the longitudinal strain and LV mass index not being significantly different. This relationship was independent of the LV mass, fibrosis amount, and LV hypertrophy pattern. This suggests that circumferential fiber dysfunction, reflecting myocyte disarray, is an important phenotype related to SM. Although LGE extent mainly affects LV myocardial function, the presence of midepicardial LGE also significantly impacts the impairment of circumferential fiber function. Our results are supported by a previous study, where patients without overt hypertrophy but with SM, showed significantly impaired circumferential strain and transmural circumferential strain differences[17]. Other interesting findings include that longitudinal strain, which reflects longitudinal fiber function in the subendocardium, was not significantly correlated with the presence of SM, but was significantly correlated with LV mass and fibrosis extent. Although longitudinal fiber dysfunction is usually observed in HCM, these findings would be mainly mediated by LV hypertrophy and fibrosis. However, our observations were not made in individuals with SM without hypertrophy; therefore, we could not conclude that longitudinal dysfunction develops before myocardial hypertrophy. Although several previous studies have demonstrated the impairment of diastolic mitral annular velocity, which reflects longitudinal fiber function, before the development of hypertrophy[18], these studies have limitations in confirming that the longitudinal fiber dysfunction is directly related to SM. Therefore, in patients with HCM, the longitudinal fiber function is affected by several structural factors.

Interestingly, the degree of basal clockwise rotation was higher in patients with SM. The underlying mechanism may be that impaired basal circumferential contraction could loosen basal free rotation within the same longitudinal subendocardial contraction. Consequently, this leads to augmented basal clockwise rotation, which is significantly associated with dynamic LVOT obstruction. Notably, this relationship remains significant even after adjusting for factors traditionally associated with LVOT obstruction, such as maximal wall thickness and size of AML. This is the first observation of LVOT obstruction related to harmonized fiber function. Therefore, basal rotation can be a sensitive index for screening and monitoring targets for medical treatments, such as beta-blockers and novel myosin inhibitors[19]. The LVOT dynamic obstruction can be alleviated by several hemodynamic conditions and medications independent of changes in AML size and maximal wall thickness. Therefore, the degree of basal rotation can vary with each hemodynamic condition and medication. Future studies investigating the relationship between the degree of rotation and trans-LVOT pressure gradient are warranted.

Patterns of LGE and SM

Myocardial fibrosis is the main pathology of HCM. Several previous studies have demonstrated that myocardial fibrosis is an essential phenotype related to SM[20], and the presence and extent of fibrosis are major risk factors for sudden cardiac death and ventricular arrhythmia contributing to structural substrates for reentry and electric heterogeneity[5]. Moreover, it is considered a potential substrate for the progression to end-stage HCM[6]. Therefore, the current guidelines for ICD implantation in the primary prevention of sudden cardiac death, emphasize the assessment of the presence and extent of LGE, which serves as a key component in risk stratification[5]. Although midwall patchy LGE at the septal-RV insertion site is a pathognomonic finding, some patients exhibited subendocardial or transmural LGE patterns. However, current guidelines do not differentiate between the patterns of LGE for risk stratification. This approach is reasonable because various causes, such as genetically driven myopathy, subendocardial ischemia, recanalized coronary embolism, or true atherosclerotic coronary artery disease, can result in tissue and electric heterogeneity. Our study confirmed that the prevalence and extent of LGE were significantly higher in the patients with SM[7,8]. In our study, we observed that the midepicardial LGE pattern was significantly related to SM, whereas the subendocardial LGE was not related to SM but showed lower prevalence in the patients with SM. Therefore, it is important to differentiate between LGE patterns to better understand their underlying origins. Although not supported by this study, the pattern of

LGE may have implications for future cardiovascular events, such as ventricular tachycardia or the progression to heart failure, whether preserved or reduced. Therefore, it needs future studies.

Study limitations

Firstly, it is important to note that the strain and rotation values obtained from feature-tracking analysis of cine CMR images may have lower absolute values compared to echocardiography owing to the lower frame rate. Secondly, the LGE patterns are variable in HCM, and some patients may exhibit both midwall patchy and subendocardial types. In this study, when a patient had any midwall patchy LGE along with the subendocardial LGE, it was classified as the midepicardial type. Thirdly, there was a time difference between CMR imaging and echocardiography, which could potentially affect the relationship between the rotation value and presence of dynamic LVOT obstruction when measured simultaneously. However, it should be noted that under stable conditions, the presence of dynamic LVOT obstruction would not easily change.

Conclusion

Circumferential myocardial function was significantly reduced in patients with SM, independent of the extent of fibrosis and hypertrophy. In contrast, longitudinal fiber function was more closely related to extent of hypertrophy and fibrosis, regardless of SM. Notably, the midepicardial LGE pattern was significantly and independently correlated with SM. We observed that dynamic LVOT obstruction was related to augmented LV basal rotation, it needs further studies. Additionally, LV diastolic function was more closely related to LV mass, the presence of LVOT obstruction, and extent of fibrosis, regardless of SM.

Data availability

The data that support the findings of this study are available on request from the corresponding author.

Received: 20 December 2023; Accepted: 1 January 2025
Published online: 04 January 2025

References

1. Kuribayashi, T. & Roberts, W. C. Myocardial disarray at junction of ventricular septum and left and right ventricular free walls in hypertrophic cardiomyopathy. *Am. J. Cardiol.* **70**(15), 1333–1340 (1992).
2. Finocchiaro, G. et al. Arrhythmogenic potential of myocardial disarray in hypertrophic cardiomyopathy: genetic basis, functional consequences and relation to sudden cardiac death. *EP Europace*. **23**(7), 985–995 (2021).
3. Sengupta, P. P. et al. Left ventricular structure and function: basic science for cardiac imaging. *J. Am. Coll. Cardiol.* **48**(10), 1988–2001 (2006).
4. Weng, Z. et al. Prognostic value of LGE-CMR in HCM: a meta-analysis. *JACC Cardiovasc. Imaging*. **9**(12), 1392–1402 (2016).
5. Ommen, S. R. et al. 2024 AHA/ACC/AMSSM/HRS/PACES/SCMR Guideline for the management of hypertrophic cardiomyopathy: a report of the American Heart Association/American College of Cardiology Joint Committee on Clinical Practice guidelines. *Circulation* **149**(23), e1239–e1311 (2024).
6. Marstrand, P. et al. Hypertrophic cardiomyopathy with left ventricular systolic dysfunction. *Circulation* **141**(17), 1371–1383 (2020).
7. Chung, H. et al. Effect of sarcomere and mitochondria-related mutations on myocardial fibrosis in patients with hypertrophic cardiomyopathy. *J. Cardiovasc. Magn. Reson.* **23**(1), 18 (2021).
8. Huang, M. et al. SARC gene mutation is associated with myocardial fibrosis measured by histopathology and cardiac magnetic resonance in patients with hypertrophic cardiomyopathy. *J. Am. Heart Association*. **12**(5), e028293 (2023).
9. Chung, H. et al. Differential contributions of sarcomere and mitochondria-related multigene variants to the endophenotype of hypertrophic cardiomyopathy. *Mitochondrion* **53**, 48–56 (2020).
10. Choi, E. Y. et al. Correction with blood T1 is essential when measuring post-contrast myocardial T1 value in patients with acute myocardial infarction. *J. Cardiovasc. Magn. Reson.* **15**(11), 15–11 (2013).
11. Park, C. H. et al. Diagnosis of acute global myocarditis using cardiac MRI with quantitative t1 and t2 mapping: case report and literature review. *Korean J. Radiol.* **14**(5), 727–732 (2013).
12. Moravsky, G. et al. Myocardial fibrosis in hypertrophic cardiomyopathy: accurate reflection of histopathological findings by CMR. *JACC Cardiovasc. Imaging*. **6**(5), 587–596 (2013).
13. Park, C. H. et al. Electrocardiography based prediction of hypertrophy pattern and fibrosis amount in hypertrophic cardiomyopathy: comparative study with cardiac magnetic resonance imaging. *Int. J. Cardiovasc. Imaging*. **34**(10), 1619–1628 (2018).
14. Whiffin, N. et al. CardioClassifier: disease- and gene-specific computational decision support for clinical genome interpretation. *Genet. Medicine: Official J. Am. Coll. Med. Genet.* **20**(10), 1246–1254 (2018).
15. Marian, A. J. Molecular genetic basis of hypertrophic cardiomyopathy. *Circul. Res.* **128**(10), 1533–1553 (2021).
16. Varnava, A. M., Elliott, P. M., Sharma, S., McKenna, W. J. & Davies, M. J. Hypertrophic cardiomyopathy: the interrelation of disarray, fibrosis, and small vessel disease. *Heart* **84**(5), 476–482 (2000).
17. Vigneault, D. M. et al. Left ventricular strain is abnormal in preclinical and overt hypertrophic cardiomyopathy: Cardiac MR Feature Tracking. *Radiology* **290**(3), 640–648 (2019).
18. Nagueh, S. F. et al. Tissue Doppler Imaging consistently detects myocardial abnormalities in patients with hypertrophic cardiomyopathy and provides a Novel means for an early diagnosis before and independently of hypertrophy. *Circulation* **104**(2), 128–130 (2001).
19. Spertus, J. A. et al. Mavacamten for treatment of symptomatic obstructive hypertrophic cardiomyopathy (EXPLORER-HCM): health status analysis of a randomised, double-blind, placebo-controlled, phase 3 trial. *Lancet* **397**(10293), 2467–2475 (2021).
20. Ho, C. Y. et al. Myocardial fibrosis as an early manifestation of hypertrophic cardiomyopathy. *N Engl. J. Med.* **363**(6), 552–563 (2010).

Acknowledgements

The authors would like to thank all of our colleagues who have contributed to this research.

Author contributions

MK, YK, and EYC made the study design and wrote the manuscript. MK, CHP, EYC and THK analyzed CMR

images and collect CMR data. HC, JS, and SJR analyzed the echocardiography. MK, JS and EYC collected the echocardiographic and clinical data. YK and KAL analyzed the genetic test results and provide critical comments on the manuscript.

Funding
This study was supported by a faculty research grant of Yonsei University College of Medicine (6-2018-0050).

Declarations

Ethics approval and consent to participate
The study protocol was approved by the Institutional Review Board of Gangnam Severance Hospital (3-2015-0019), and informed consent was obtained from all participants. The study was performed in accordance with relevant guidelines/regulations and the Declaration of Helsinki.

Consent for publication
All the authors read a final version of manuscript and approved for publication.

Competing interests
The authors declare no competing interests.

Additional information
Supplementary Information The online version contains supplementary material available at https://doi.org/10.1038/s41598-025-85201-0.

Correspondence and requests for materials should be addressed to K.-A.L. or E.-Y.C.